Biogeosciences, 18, 189–205, 2021
https://doi.org/10.5194/bg-18-189-2021

Biogeosciences
Open Access
EGU

Millennial-age glycerol dialkyl glycerol tetraethers (GDGTs) in forested mineral soils: ^{14}C-based evidence for stabilization of microbial necromass

Hannah Gies[1], Frank Hagedorn[2], Maarten Lupker[1], Daniel Montluçon[1], Negar Haghipour[1,3], Tessa Sophia van der Voort[4], and Timothy Ian Eglinton[1]

[1]Department of Earth Sciences, ETH Zurich, Sonneggstrasse 5, 8092 Zurich, Switzerland
[2]Swiss Federal Institute for Forest, Snow and Landscape Research (WSL), Zürcherstrasse 111, 8903 Birmensdorf, Switzerland
[3]Laboratory of Ion Beam Physics, ETH Zurich, Otto-Stern-Weg 5, 8093 Zurich, Switzerland
[4]Campus Fryslân, Rijksuniversiteit Groningen, Wirdumerdijk 34, 8911 CE Leeuwarden, the Netherlands

Correspondence: Hannah Gies (hannah.gies@erdw.ethz.ch)

Received: 11 August 2020 – Discussion started: 26 August 2020
Revised: 2 November 2020 – Accepted: 21 November 2020 – Published: 12 January 2021

Abstract. Understanding controls on the persistence of soil organic matter (SOM) is essential to constrain its role in the carbon cycle and inform climate–carbon cycle model predictions. Emerging concepts regarding the formation and turnover of SOM imply that it is mainly comprised of mineral-stabilized microbial products and residues; however, direct evidence in support of this concept remains limited. Here, we introduce and test a method for the isolation of isoprenoid and branched glycerol dialkyl glycerol tetraethers (GDGTs) – diagnostic membrane lipids of archaea and bacteria, respectively – for subsequent natural abundance radiocarbon analysis. The method is applied to depth profiles from two Swiss pre-Alpine forested soils. We find that the Δ^{14}C values of these microbial markers markedly decrease with increasing soil depth, indicating turnover times of millennia in mineral subsoils. The contrasting metabolisms of the GDGT-producing microorganisms indicates it is unlikely that the low Δ^{14}C values of these membrane lipids reflect heterotrophic acquisition of ^{14}C-depleted carbon. We therefore attribute the ^{14}C-depleted signatures of GDGTs to their physical protection through association with mineral surfaces. These findings thus provide strong evidence for the presence of stabilized microbial necromass in forested mineral soils.

1 Introduction

Soil organic matter (SOM) represents the largest reservoir of carbon in terrestrial ecosystems, exchanging large quantities of carbon with the atmosphere and supplying aquatic systems with organic and inorganic C (Parry et al., 2007; Battin et al., 2009; Bradford et al., 2016). SOM is comprised of a complex mixture of components that turn over on a wide range of timescales (from seconds to millennia), introducing large uncertainties in climate model predictions (Carvalhais et al., 2014; He and Yu, 2016). Emerging concepts of SOM suggest that only a small fraction of annual C inputs from plants persists in the soils, and that microbial products and residues stabilized by the interaction with reactive minerals comprise the majority of the soil C pool (Schmidt et al., 2011; Cotrufo et al., 2015; Lehmann and Kleber, 2015; Kallenbach et al., 2016; Kästner and Miltner, 2018). Correspondingly, microbial processes are increasingly being incorporated into soil carbon cycle models (Riley et al., 2014; Ahrens et al., 2015). However, evidence of the entombment of microbial necromass is presently limited and largely circumstantial, being primarily based on the finding of increasing contributions of microbial biomarkers compared to plant-derived compounds with increasing soil depth (Amelung et al., 2008; Miltner et al., 2012; Kallenbach et al., 2016; Liang et al., 2019; Ma et al., 2018).

Radiocarbon provides valuable constraints on carbon turnover in soils (Trumbore et al., 1996; Schrumpf and Kaiser, 2015), and ^{14}C measurements are particularly useful when applied at the level of specific compounds (e.g., Van der Voort et al., 2017). Prior ^{14}C analyses of plant-derived biomarkers have indicated their stabilization in mineral soils (Huang et al., 1999; van der Voort et al., 2016), but ^{14}C-based evidence for stabilization of microbial necromass in SOM is currently lacking. $\Delta^{14}C$ signatures of fatty acids and phospholipid fatty acids (PLFAs), established indicators for plant and microbial-derived C, suggest active microbial resynthesis of lipids in deeper soil (Matsumoto et al., 2007; Gleixner, 2013) rather than the stabilization of microbial necromass (Kramer and Gleixner, 2008).

Here we examine the ^{14}C characteristics of glycerol dialkyl glycerol tetraethers (GDGTs) – characteristic membrane lipids of microorganisms that are ubiquitous in terrestrial and aqueous environments (Schouten et al., 2013). GDGTs are subdivided into two groups of compounds, namely isoprenoid GDGTs (isoGDGTs), produced by archaea (De Rosa and Gambacorta, 1988), and branched GDGTs (brGDGTs), which are of putative bacterial origin (Weijers et al., 2006a) and are especially abundant in soils and peats (Weijers et al., 2006b). For molecular structures, see Fig. A1. GDGTs have garnered much attention due to their potential as molecular proxies for environmental conditions; the relative abundance of brGDGTs versus isoGDGTs has been used to qualitatively estimate soil-derived carbon input into marine sediments (Hopmans et al., 2004), while the internal distribution of iso- and brGDGT isomers carries information on aquatic and soil conditions (e.g., Schouten et al., 2002; Powers et al., 2004, 2010; Liu et al., 2013; Coffinet et al., 2014; Yang et al., 2016). For example, the distribution of different brGDGTs, parameterized as the methylation of branched tetraethers (MBTs) and cyclization of branched tetraethers (CBTs) indices (Peterse et al., 2012; De Jonge et al., 2014a; Naafs et al., 2017), has been found to correlate with mean annual continental air temperature (MAT) and soil pH (Weijers et al., 2007), respectively.

Despite their rapid adoption by biogeochemists and paleoclimatologists as molecular tracers and proxies of environmental conditions, there are numerous aspects regarding their production, turnover and fate that remain enigmatic. While isoGDGTs in soils are most likely produced by ammonia-oxidizing Crenarchaeota and heterotrophic methanogens (Weijers et al., 2010), the biological precursors, metabolic processes and physiological drivers giving rise to brGDGT signatures observed in terrestrial and aquatic systems remain poorly constrained, despite their ubiquity in soils and other environmental matrices. The bacteria that produce brGDGTs are supposedly heterotrophs (Pancost and Damsté, 2003; Weijers et al., 2010; Colcord et al., 2017). Acidobacteria have been suggested as potential precursor organisms (Weijers et al., 2009; Sinninghe Damsté et al., 2011), though other phyla cannot be excluded (Sinninghe Damsté et al., 2018).

Previous estimations of the turnover time of GDGTs in soils have been based on stable isotopes and incubation experiments (Weijers et al., 2010; Huguet et al., 2017). Corresponding turnover times are of the order of a few decades, and similar to those of other plant and microbial biomarkers (Schmidt et al., 2011), but these approaches tend to reflect turnover of the new carbon inputs from plants and yield faster SOM turnover rates than ^{14}C-based estimates that measure overall organic matter turnover (Trumbore, 2000). Moreover, the focus of these studies has been on the SOM-rich upper soil horizons and may obscure slow-cycling carbon pools that predominate at depth (Rumpel and Kögel-Knabner, 2011). In this context, natural-abundance-level radiocarbon measurements of these compounds may provide a valuable approach to better understand their source(s) and turnover rates, while also shedding light on processes that influence their abundance and distribution (Mendez-Millan et al., 2014; Van der Voort et al., 2017).

Prior ^{14}C-based studies of GDGTs have primarily focused on the isoprenoid compounds in marine waters and sediments (Pearson et al., 2001; Smittenberg et al., 2004; Ingalls et al., 2006; Mollenhauer et al., 2007, 2008; Shah et al., 2008). The only reported investigation of brGDGT ^{14}C characteristics in lake sediments (Birkholz et al., 2013) yielded $\Delta^{14}C$ values that were lower than those of the depositional age of the sediment, although the causes of this preaged signal was not established. In soils, however, attempts to determine the ^{14}C signature of GDGTs are rare (Courel et al., 2015). Thus, we presently lack crucial information concerning the production and cycling of this distinctive group of microbial lipids in the context of soil C cycling and the implications for their use as molecular tracers and proxies.

In the present study, we used molecular-level, natural-abundance ^{14}C measurements to constrain the provenance and turnover of GDGTs in soils. We developed and rigorously tested a preparative high-performance liquid chromatography (HPLC) method to isolate both isoGDGTs and brGDGTs from soils (and sediments) for subsequent small-scale radiocarbon analysis by accelerator mass spectrometry (AMS). We then applied this method to samples from two well-studied sub-Alpine Swiss soil profiles in order to shed light on their origin and stability. As unequivocal markers of microbial contributions to soils, the GDGTs provide an opportunity to assess the stability and turnover of microbial biomass in soils.

2 Methods

2.1 Study site

Soils were sampled by taking soil cores at two forested sites in Switzerland, namely one near Lausanne (46.5838° N, 6.6580° E; 800 m above sea level – a.s.l.) and the other one close to Beatenberg (46.7003° N, 7.7623° E; 1490 m a.s.l.;

locations of both sites are displayed in Fig. 3). Both sites are both part of the Long-term Forest Ecosystem Research (LWF) network (Innes, 1995) maintained by the Swiss Federal Institute for Forest, Snow and Landscape Research (WSL).

The sub-Alpine soil from the site at Beatenberg is a podzol, which has a thick organic layer followed by a 10 cm A horizon and carbonate-free sandstone as parent material. The MAT at the site is 4.6 °C, and the pH rises from 3.7 to 4.4 with increasing soil depth. The second soil from the Swiss Plateau close to Lausanne is a Cambisol developed on top of a carbonate-containing moraine. Its A horizon extends to 50 cm, with a total soil depth of 3 m. Here, the MAT is 7.6 °C, and the pH is slightly higher compared to the Beatenberg soil and largely invariant (4.6 to 4.5) to a depth of 80 cm (Walthert, 2003).

At each site, soil cores were taken from 16 locations on a regular grid on a 1600 m^2 plot, following protocols implemented as part of the LWF sampling program (van der Voort et al., 2016), and bulked to yield representative samples for three depth layers at each site as follows: a sample from the A horizon comprising the top 5 cm of the soil, a second ranging from 10 to 20 cm depth and a third from the B horizon at 20 to 40 and 60 to 80 cm depth at the Beatenberg and Lausanne site, respectively. These soil composites have been previously analyzed for radiocarbon signatures of organic carbon in bulk soil and soil density fractions, and in specific alkanes and fatty acids (Van der Voort et al., 2017), which allows the comparison of the isoprenoid and branched GDGTs with other biomarkers and operationally defined soil carbon pools.

2.2 Reference materials for method validation

Evaluation of the isolation method involved an assessment of the purity of separated fractions (i.e., potential interference from compounds other than the desired compounds) and determination of the amount and isotopic composition of external contamination introduced in course of the preparation sequence. For the latter, composites of different topsoil samples (0–5 cm) from a 30×30 m grassland area in central Switzerland (5.9 % C; bulk $F^{14}C = 1.155$) and a Rhineland lignite from the early Miocene (Heumann and Litt, 2002) (62.3 % OC; bulk $F^{14}C = 0.003$) were used for assessment and validation with regard to contamination.

2.3 GDGT isolation for radiocarbon measurement

Despite the relative ease of detection of GDGTs using modern HPLC mass spectrometry (MS) techniques, one challenge in the radiocarbon analysis of GDGTs in soil and sediment samples is their low abundance, with ambient concentrations of brGDGTs and isoGDGTs that are typically in the range of 10 to 1000 and 1 to 100 ng gdw^{-1} (grams of dry weight) soil, respectively (Weijers et al., 2006b). A separation of individual GDGTs in the soil samples used in this study would require, on average, 3000 g of soil to reach the minimum recommended mass (~ 15 µg C) for high-precision, compound-specific radiocarbon analysis (Haghipour et al., 2018). As extracting several kilograms of material is impractical, we did not attempt to isolate individual molecules (Fig. A1) but focused instead on pooled isolation and ^{14}C measurement of isoprenoid GDGTs and branched GDGTs, respectively, at the compound class level, due to the common putative biological precursors and biosynthetic formation pathways for each compound class (Schouten et al., 2013). For this study, the pooling of the GDGTs reduced the required initial sample size to a maximum of 500 gdw of soil. The extraction and purification of the compounds prior to the HPLC analysis followed a procedure that is similar to that applied to samples processed for quantification of GDGTs (Freymond et al., 2017). In brief, lipids were extracted from dried soil samples using a microwave (CEM MARS 5) or an energized dispersive guided extraction (CEM EDGE) system. No difference in performance was observed for the different extraction systems. Samples were processed in batches of roughly 15 to 20 g of material. For microwave extraction, the samples were transferred to the extraction vessels and covered by a dichloromethane (DCM) and methanol (MeOH) 9 : 1 (v/v; 25 mL) solvent mixture. Extraction temperature was programmed to ramp to 100 °C in 35 min and was subsequently held for 20 min. For EDGE extraction, 25 mL DCM : MeOH 9 : 1 (v/v) was used for extraction at 110 °C for 2 min and subsequent rinsing with 15 mL, followed by a second extraction with 5 mL of solvent at 100 °C and rinsing with 35 mL. The process was repeated on additional sample batches to yield sufficient quantities of the target lipid compounds for ^{14}C analysis. Pooled extracts were then dried under nitrogen flow. After the addition of 5 mL Milli-Q water with NaCl, the neutral phase was back-extracted with hexane (Hex) and separated on a 1 % deactivated silica column into apolar and polar fractions with Hex : DCM 9 : 1 (v/v) and DCM : MeOH 1 : 1 (v/v), respectively. Polar fractions were dried under N_2, then redissolved in Hex : 2-propanol (IPA) 99 : 1 (v/v) and passed over 0.45 µm polytetrafluoroethylene (PTFE) filters. A portion of the polar fraction was set aside (1 %) and an internal C_{46} GDGT standard (Huguet et al., 2006) was added to this aliquot to determine GDGT concentrations.

Polar fractions were separated on an Agilent 1260 HPLC system coupled to an Agilent 1260 fraction collector. Separation was achieved on two Waters Acquity UHPLC HEB hydrophilic liquid interaction chromatography (HILIC) columns (1.7 µm; 2.1×150 mm) connected in a series and preceded by a 2.1×5 mm guard column (Hopmans et al., 2016). The columns were heated to 45 °C and the flow rate set to 0.2 mL min^{-1}. For the first 25 min, compounds elute isocratically with a solvent mixture of 18 % Hex : IPA 9 : 1 (v/v; solvent A) and 82 % hexane (solvent B). For the next 15 min, the proportion of solvent B was decreased linearly

to 65 %, followed by a linear gradient to 0 % solvent B in 20 min. The total runtime of one injection hence adds up to 60 min, followed by 20 min reequilibration with 82 % solvent B. The fraction collection is solely based on retention times, with the isoprenoid fraction being collected from 14.5 to 26 min and the branched fraction from 33 to 43 min (Fig. 1). The retention time is recurrently monitored to avoid undetected drifts. The injection volume is set to 15 µL, corresponding to total GDGT amounts of 100 to 300 ng mL^{-1}. Each sample was injected 10 times, and fractions were pooled afterwards. The isolated compound classes and the subset of the initial polar fraction set aside previously were analyzed for purity and quantification using the same HPLC system coupled to a quadrupole mass spectrometer (Agilent 6130), according to Hopmans et al. (2016), with the exception that the purity of the isolated fractions was tested in full scan instead of selected ion-monitoring mode. The isolated fractions were dried and transferred into 0.025 mL tin capsules (Elementar 03951620). The capsules containing each sample were measured using an elemental analyzer coupled to a gas-ion-source equipped accelerator mass spectrometer (EA-AMS) (Haghipour et al., 2018) at the Laboratory of Ion Beam Physics (LIP) at ETH Zurich (Synal et al., 2007; Ruff et al., 2007). In all cases, sample sizes were > 15 µg C.

2.4 Soil turnover model

Even at the compound scale, SOM cycles on a continuum of timescales (Sollins et al., 1996; Feng and Simpson, 2008). Hence, turnover times of the individual compounds are calculated based on a steady-state, two-pool box model (e.g., Trumbore et al., 1996; Torn et al., 2009; Schrumpf and Kaiser, 2015; van der Voort et al., 2019). This model assumes two homogeneous pools with a first-order decay rate, namely a fast-cycling pool and a passive pool. For each of the pools, the $F^{14}C$ is calculated independently (Eq. 1), where $F^{14}C_{pool(t)}$ is the radiocarbon signal of the respective pool in the sampling year t, lag is the number of years between CO_2 fixation in plants and plant litter entering the soil, λ is the radioactive decay of ^{14}C (1/8267 years) and k_{pool} is the decomposition rate constant.

$$F^{14}C_{pool(t)} = F^{14}C_{atm(t\text{-lag})} \cdot k_{pool} + F^{14}C_{pool(t-1)} \cdot (1 - k_{pool} - \lambda) \quad (1)$$

The fraction-weighted sum of the $F^{14}C$ of each of the pools is the modeled $F^{14}C$ of the sample and depends on the decomposition rate constants of each pool, k_1 and k_2, and the relative size of the two pools. The $\Delta^{14}C$ of atmospheric CO_2 was taken from Hua et al. (2013) from 1950 to 1986 and from Hammer and Levin (2017) for the years thereafter.

3 Results

3.1 Method validation

Repetitive preparation of samples with 10 injections each reveals a recovery efficiency of 0.85 ± 0.05. Analysis of isolated fractions on a quadrupole mass spectrometer operated in scan mode (Agilent 6130) for all masses between *m/z* 500 and 1500 reveals that more than 95 % of compounds in either fraction are comprised of masses assigned to GDGTs (Fig. 1).

The extraneous contamination added in the preparatory process is assumed to be of constant mass m_c and radiocarbon signature $F^{14}C_c$. Therefore, the measured signal $F^{14}C_m$ is a mixture of the sample and the contaminant, according to Eq. (2) as follows:

$$F^{14}C_m = \frac{F^{14}C_s \cdot m_s + F^{14}C_c * m_c}{m_s + m_c} \quad (2)$$

$F^{14}C_s$ and m_s are the true radiocarbon signal and carbon mass of the sample. The measured $F^{14}C_m$ changes, depending on the mass of the sample, as smaller masses are more strongly affected by the constant contamination. We assume that, in samples with a bulk radiocarbon signal that is either completely modern or does not contain any ^{14}C at all, the compound-specific radiocarbon value is similar to the bulk. Therefore, a radiocarbon-modern sample, i.e., the topsoil composite, and the radiocarbon-dead lignite were prepared and measured repeatedly with different concentrations. The best fit for $F^{14}C_c$ and m_c, to match the observed $F^{14}C_m$ for both sets of measurements, is calculated according to Haghipour et al. (2018).

The blank assessment (Fig. 2) yields a contamination of 2.62 ± 0.79 µg C, with a fraction modern of 0.59 ± 0.18, which is in range of previously determined contamination introduced by HPLC separation of lipids (e.g., Shah and Pearson, 2007; Birkholz et al., 2013). The impact of the constant contamination decreases as the sample mass increases. Therefore, the limit towards large carbon masses of the fitted curve is equivalent to the radiocarbon signal of the sample unaffected by extraneously introduced carbon. For both samples, this limit and hence the compound $F^{14}C$ differs from the bulk $F^{14}C$ of the initial material. In the topsoil reference, the compounds are depleted in radiocarbon ($F^{14}C = 0.94$) with respect to the source; in the lignite, the GDGTs are enriched ($F^{14}C = 0.06$).

The recommended sample size to reach a precision of < 5 % varies depending on the age of the sample. For samples with a radiocarbon age of < 1800 years ($F^{14}C > 0.8$), a size of 20 µg C is sufficient to reach the desired precision, while samples older than 6000 years ($F^{14}C > 0.5$) require at least 50 µg C. These uncertainties are taken into account when considering the GDGT ^{14}C results for the soil samples measured in this study.

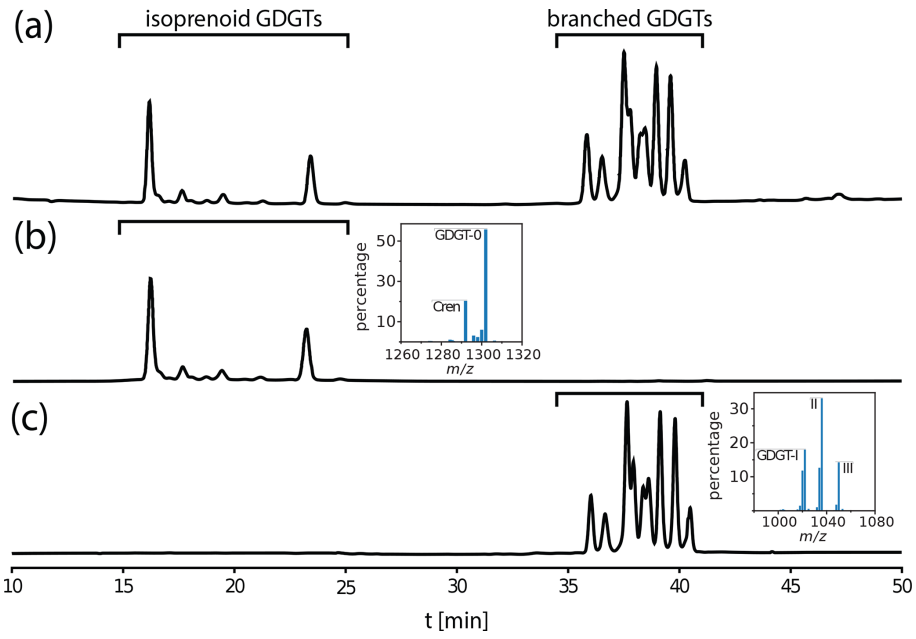

Figure 1. High-performance liquid chromatography (HPLC) mass chromatograms (m/z 500–1500) of glycerol dialkyl glycerol tetraethers (GDGTs) from a composition topsoil sample. **(a)** Sample before GDGT isolation. **(b)** The separated isoprenoid fraction and its composite mass spectrum (GDGT-3, GDGT-2 and GDGT-1, from left to right, between Crenarchaeol (Cren) and GDGT-0, which are not labeled). **(c)** The separated branched fraction and its composite mass spectrum (GDGT-I, II and III corresponding to tetra-, penta- and hexamethylated GDGTs, which are labeled). For molecular structures, see Fig. A1.

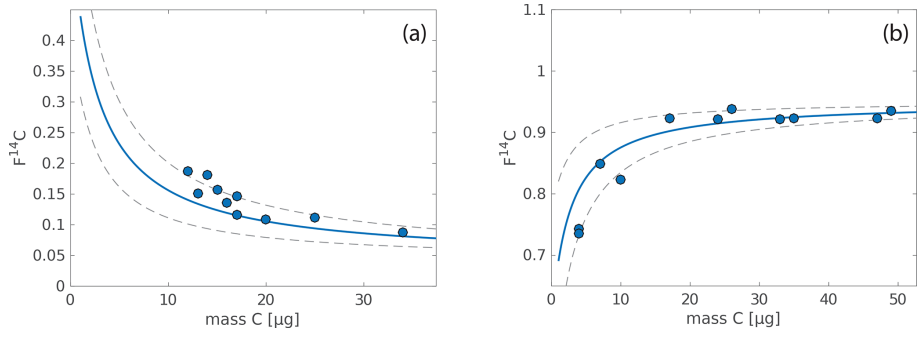

Figure 2. Blank assessment associated with GDGT isolation. **(a)** The $F^{14}C$ dead standard (lignite) tracing a modern constant contamination of 1.55 µg C. **(b)** The $F^{14}C$ modern standard (topsoil composite) tracing a radiocarbon dead constant contamination of 1.07 µg C. The solid line indicates the best fit of contamination mass and radiocarbon signal for both sets of samples considered jointly. The gray dotted lines show the 1σ error range.

3.2 Vertical distributions of GDGTs

In the Lausanne soil, concentrations of GDGTs are generally highest in the topsoil, where the isoprenoid and branched GDGTs comprise 0.6 and 2 µg gdw^{-1}, respectively, whereas corresponding concentrations in the topsoil layer of the Beatenberg soil are much higher, at 10 and 38 µg gdw^{-1}, respectively (Fig. 3). The concentration of both groups of GDGTs decreases sharply with increasing soil depths, with approximately 10 times the abundance of isoGDGTs and brGDGTs in the top 5 cm than in a few centimeters below. In contrast, iso- and brGDGT concentrations normalized to organic carbon (OC) content increase with depth in the Beatenberg soil from 47 µg gOC^{-1} for isoGDGTs and from 175 µg gOC^{-1} for brGDGTs in the top 5 cm to 273 and 80 µg gOC^{-1}, respectively, between 20 and 40 cm depth. In the Lausanne soil profile, the OC-normalized isoprenoid and branched concentrations drop from 10 and 39 µg gOC^{-1}, respectively, in the top 5 cm to 4 and 13 µg gOC^{-1} between 10 and 20 cm depth, and then increase to 14 and 12 µg gOC^{-1} between 60 and 80 cm.

Changes in the relative abundance of the individual brGDGTs (Fig. A1) are reflected in the methylation of branched tetraethers (MBT'_{5Me}) index and in the cyclization

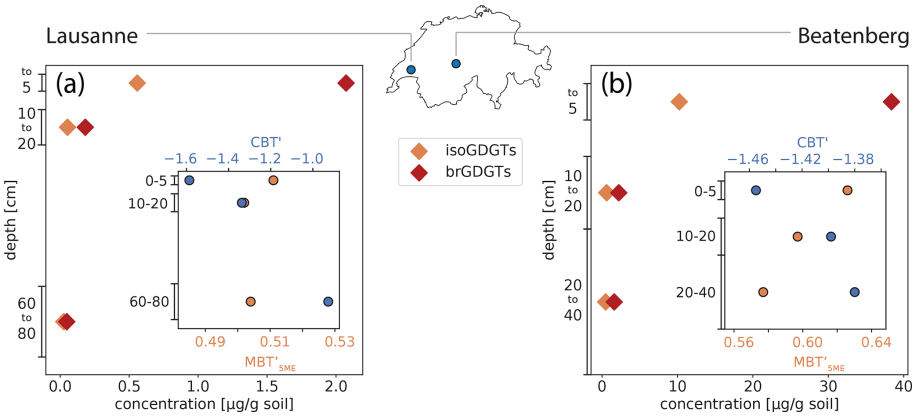

Figure 3. Branched GDGT (brGDGT) abundances and parameter ratios in Lausanne and Beatenberg soil profiles. In both soils (**a** – Lausanne; **b** – Beatenberg), the concentration of the samples per dry weight decreases rapidly with depth. The inner plots show the brGDGT-derived MBT'_{5ME} (orange) and the CBT' (blue) indices in the respective soil. While the MBT'_{5ME} does not vary a lot with depth, the CBT' increases significantly with depth in the Lausanne soil.

of branched tetraethers (CBT') index, with these parameters increasing with higher proportions of methyl groups and cyclopentane moieties, respectively, in the brGDGT structures (De Jonge et al., 2014a). In the Lausanne soil, the MBT'_{5Me} is largely invariant with depth, while the CBT' increases from -1.59 to -0.93 (Fig. 3), indicating a higher proportion of GDGTs with cyclopentane moieties in the subsoil. In the Beatenberg soil, a more modest increase in the CBT' index is evident, with a change from -1.46 to -1.38, while the MBT'_{5Me} decreases slightly from 0.63 to 0.58.

3.3 Radiocarbon variations

The GDGT fractions prepared for AMS measurement contained between 30 and 80 µg C, except for the brGDGTs in the 10 to 20 cm depth interval in Beatenberg and the iso- and brGDGTs from 60 to 80 cm the Lausanne soil, which range between 15 and 20 µg C. The results of the radiocarbon measurements are shown in Fig. 4, together with previously reported ^{14}C data for other soil carbon constituents (Van der Voort et al., 2017) .

In the Lausanne profile, $\Delta^{14}C$ values of iso- and brGDGTs decrease with depth from -20 and -7 ‰ at 0 to 5 cm to -441 and -310 ‰ at 60 to 80 cm, respectively. GDGT $\Delta^{14}C$ values are systematically lower than bulk OC at each depth interval, with the difference between GDGTs and bulk OC ranging from -105 to -200 ‰. This contrasts with dissolved organic carbon (DOC), which exhibits ^{14}C-enriched and relatively invariant $\Delta^{14}C$ values throughout the soil profile (24 ‰ in the topsoil to -58 ‰ in the deeper soil; Fig. 4). The GDGT $\Delta^{14}C$ values are also more depleted than those of short-chain (C_{16-22}) fatty acids (FAs) in the soil, but are bracketed by n-C_{27} n-alkane and n-C_{28} fatty acid $\Delta^{14}C$ values in the deepest soil section (Van der Voort et al., 2017).

Similar patterns exist in the Beatenberg profile. Radiocarbon signatures of both iso- and brGDGTs decrease with $\Delta^{14}C$ values of -23 ‰ and -30 ‰, respectively, in the top 5 cm to -241 ‰ and -196 ‰ in the 20 to 40 cm depth interval, respectively. While $\Delta^{14}C$ values of bulk OC and GDGTs show a systematic offset in the Lausanne soil, GDGT and bulk OC $\Delta^{14}C$ values parallel each other closely in the Beatenberg profile (Fig. 4). Overall, $\Delta^{14}C$ values of both groups of GDGTs are similar to those of a C_{29} n-alkane and the long-chained ($> C_{26}$) n-alkanoic FAs, but differ sharply from those of DOC and shorter-chained FAs (C_{16}–C_{22}) measured on the same samples (Van der Voort et al., 2017). The latter never reach $\Delta^{14}C$ values lower than -90 ‰ in the soils, resulting in an offset between short-chained FAs and the other analyzed compounds that show stronger decreases with soil depth.

The $\Delta^{14}C$ values of the density fractions from the same soil samples were also measured by Van der Voort et al. (2017). The low-density fraction corresponds to the free particulate organic carbon (free POC) and the high-density fraction is interpreted as mineral-associated POC. Both fractions do not differ by more than 40 ‰ in the top 20 cm of either soil profile, but in the lowest depth interval the fractions diverge, with markedly lower $\Delta^{14}C$ values the for high-density fraction and values similar to DOC for the free POC fraction. In both soils, the iso- and brGDGTs exhibit similar or lower $\Delta^{14}C$ values than the high-density fraction and mineral-associated organic matter fraction.

3.4 Radiocarbon derived turnover times of GDGTs

Turnover times of the compounds are calculated based on a two-pool model that requires the following three parameters to be fitted: the turnover time of the fast-cycling pool, the turnover time of the passive pool and the proportion of the fast-cycling pool. As only one radiocarbon measurement per compound and depth interval is available, two of the parameters need to be estimated, while one can be fit-

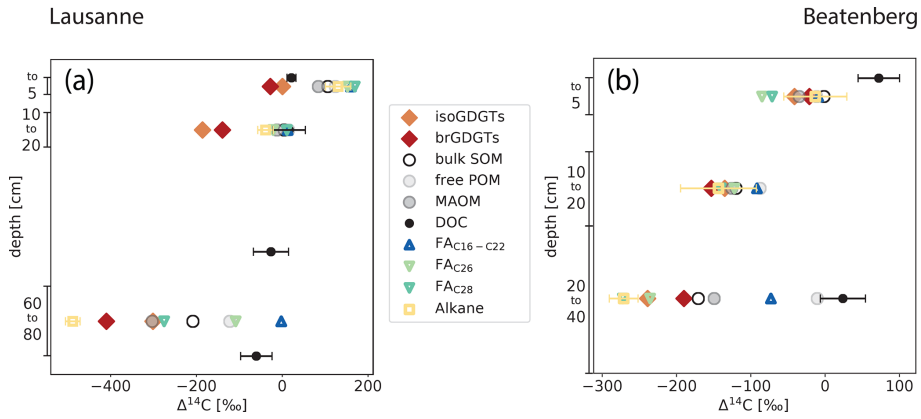

Figure 4. Radiocarbon content expressed as $\Delta^{14}C$ of organic matter fractions and compounds in Lausanne and Beatenberg soil profiles. In both soils (Lausanne – **a**; Beatenberg – **b**), the radiocarbon contents of both branched and isoprenoid GDGTs decrease to a similar degree to that of bulk SOM in each profile. The measured *n*-alkane in the Beatenberg soil is C_{29}; in the Lausanne soil the *n*-C_{27} homologue was analyzed. Alkane, *n*-fatty acid (FA), free particulate organic matter (POM), mineral-associated organic matter (MAOM) and dissolved organic carbon (DOC) $\Delta^{14}C$ values are taken from Van der Voort et al. (2017). DOC was not measured in the same intervals as the other parameters but at 0, 15, 50 and 80 cm and at 0 and 30 cm depth in the Lausanne and Beatenberg soils, respectively. If error bars are not visible, then the uncertainty is smaller than the symbol size.

ted accordingly. We use the proportion of the low-density particulate organic matter consisting of some decomposed residues, the so-called light fraction of the samples (Van der Voort et al., 2017), to constrain the size of the fast-cycling pool. The turnover time of the fast-cycling pool can be estimated accordingly as the single-pool turnover time of this light fraction. Alternatively, the GDGT turnover in topsoil, based on stable carbon isotopes, has been shown to be similar to short-chain fatty acids (Weijers et al., 2010; Huguet et al., 2017). Thus, the turnover time of these compounds based on a single-pool box model can also be used to constrain the turnover time of the fast-cycling pool of GDGTs. For simplicity, a lag term addressing the time between atmospheric carbon fixation and input into the soil is not used, as it is shorter than a decade (Solly et al., 2018), and its potential influence is hence already covered by the range of the turnover time estimates of the fast pool (Table 1. The resulting GDGT turnover times, based on either short-chain FAs or the light fraction, differ by less than 5 %. The low $\Delta^{14}C$ values of GDGTs in the deeper soil intervals result in a turnover time of the passive GDGT pool of the order of 1400 to 2000 years between 10 and 20 cm depth and 2000 up to 6000 years in the lowest depth interval in either soil (Table 1). These results are insensitive to changes in either the turnover time and the size of the labile pool. A change of ±10 % of the proportion of the fast pool or ±500 years of the turnover time of the fast pool results in a maximum change of 10 % of the overall GDGT turnover time in the two lower depth intervals in either soil. Thus, despite the uncertainties in the estimation of the proportion of the pools and the turnover time of the fast pool, the turnover time of both groups of GDGTs clearly exceeds a millennium.

4 Discussion

4.1 Efficacy of GDGT isolation and ^{14}C measurement protocol

Compared to prior methods used to achieve individual isoGDGT separation by HPLC (Smittenberg et al., 2002; Ingalls et al., 2006), the introduced method isolates GDGTs only at the compound-class level; hence, potential radiocarbon variations among GDGT isomers are not discernable. However, previous analyses of stable carbon isotopic and radiocarbon analysis of GDGTs on a molecular level do not show significant differences between the individual isoprenoid or branched GDGTs, respectively (e.g., Ingalls et al., 2006; Shah et al., 2008; Oppermann et al., 2010; Weber et al., 2015). This implies similar metabolisms for brGDGT-producing organisms and also for microbial communities that synthesize isoGDGTs. Consequently, pooling of isomers within a compound class according to their respective microbial domain (bacteria and archaea) seems reasonable, particularly given the practical constraints imposed by their low abundance in many terrestrial (and aquatic) environments. The introduced method requires only a single normal-phase isolation step, using the same columns that are used for quantification of GDGTs (Hopmans et al., 2016), minimizing the time required for sample preparation and without extensive adjustments to the analytical HPLC setup. The calculated contamination is in the range of the blank assessment by Ingalls et al. (2006) but higher than the extraneous carbon observed by Birkholz et al. (2013). However, the blank assessment in Birkholz et al. (2013) is based only on a modern non-GDGT standard (cholesterol), potentially leading to an underestimation of the sample preparation blank.

Table 1. Turnover times of isoprenoid and branched GDGTs. Turnover times are based on the single-pool turnover time of the light fraction (fPOM) or the short-chain fatty acids (SCFA – in parentheses) as approximation of the fast pool. Note: Loc – location.

		Fast pool	Turnover times fPOM (SCFA); (years)					
Loc	Depth	proportion	Fast pool		isoGDGT		brGDGT	
Bb	0–5 cm	0.897	350	(340)	710	(740)	440	(450)
	10–20 cm	0.193	890	(920)	1400	(1400)	1600	(1600)
	20–40 cm	0.115	350	(760)	2800	(2700)	2100	(2000)
Ln	0–5 cm	0.162	46	(33)	350	(360)	540	(550)
	10–20 cm	0.113	240	(240)	2000	(2000)	1400	(1400)
	60–80 cm	0.087	1200	(300)	3600	(3700)	5900	(6100)

The GDGT-specific $\Delta^{14}C$ values of the topsoil and lignite samples used as modern and fossil end-members for blank assessment did not yield values that fully matched those expected given their age. In the case of the soil, different $\Delta^{14}C$ values of the GDGTs compared to bulk OC are to be expected due to the heterogeneous nature of soil organic matter; however, for a lignite sample that is of geologic age (> 30 Ma), all components would be expected to be radiocarbon dead. A preliminary batch of lignite that was extracted yielded 18 µg C of isoGDGTs and 48 µg C of brGDGTs, with corresponding $\Delta^{14}C$ values of the resulting isolated compounds of -960 ‰ and -980 ‰, respectively. The second batch of lignite used to assess constant contamination was prepared 4 months later and shows $\Delta^{14}C$ values consistently higher than -950 ‰ (Fig. 2). This shift towards higher $\Delta^{14}C$ values likely reflects contamination resulting from sample-to-sample carryover on the HPLC. Although this is addressed in the blank assessment, this highlights the importance of repeated blank assessment in order to control for variations in carryover and other potential sources of contamination (e.g., column bleed) over time. Careful assessment of compound purity is also important to ensure robust isotopic determination.

4.2 Radiocarbon constraints on the origin and turnover of GDGTs in soils

Our study reveals low $\Delta^{14}C$ values, with corresponding radiocarbon ages of up to 6000 years for GDGTs in forested soils. These ^{14}C characteristics are similar to those of the mineral-associated OM (from density fractionation) and long-chain, higher plant-wax-derived *n*-fatty acids and *n*-alkanes. As GDGTs are microbial membrane lipids, these findings reveal the presence of ^{14}C-depleted, millennial-age microbial residues as a component of organic matter in deeper soils. There are two possible pathways leading to these old apparent radiocarbon ages, namely that (1) active GDGT-producing heterotrophic soil microbial communities in deeper soils are utilizing preaged SOM as a carbon source and accrue this signal with continuous community turnover. Alternatively, (2) upon cell death these microbial lipids are stabilized for millennia, likely via interaction with soil minerals. We first consider the first explanation in the following.

The $\Delta^{14}C$ values of living organisms, and their constituent lipids, directly reflect the $\Delta^{14}C$ values of their metabolic carbon source as they are corrected for biological fractionation effects (Ingalls and Pearson, 2005). Upon the death of the organism, radioactive decay leads to depletion in ^{14}C contents. Consequently, the ^{14}C contents of iso- and brGDGTs should reflect that of the carbon source of their biological precursors. IsoGDGTs are known to be produced by Thaumarchaeota and Euryarchaeota (Schouten et al., 2013). The specific microbes that produce brGDGTs are yet to be identified; however, there is strong evidence that the precursor organisms are heterotrophic bacteria (Pancost and Damsté, 2003; Weijers et al., 2010), with Acidobacteria amongst the candidate phyla (Sinninghe Damsté et al., 2018). For heterotrophic bacteria, potential carbon sources include DOC leached from the organic layer, exudates from root systems or organic matter that has accumulated during soil development. The activity of soil microbial communities has often been assayed using phospholipid fatty acids (PLFAs), as phospholipids are only found in living cells and thus serve as biomarkers for viable microbial communities (e.g., Tunlid and White, 1991). Compound-specific radiocarbon analyses of PLFAs have shown that soil microbes can use a variety of carbon sources, including older SOM (Kramer and Gleixner, 2006). However, root-derived C seems a dominant food source of heterotrophic microbial communities in temperate deciduous forest soils (Kramer et al., 2010), and this has been inferred to be a likely substrate for the producers of brGDGTs (Huguet et al., 2013). The turnover time of root carbon is of the order of decades at most Gill and Jackson, 2000; Gaudinski et al., 2001; Solly et al., 2018), and thus the old ages and long turnover times of GDGTs observed in both soils analyzed in this study cannot be explained by the uptake of root-derived C. Accessible, labile carbon pools in the investigated soil profiles are represented by DOC and the light density fraction. These appear to be preferably used by microbial communities as evidenced by the ^{14}C-enriched values of short-chain ($< C_{24}$) fatty acids that likely reflect active microbial communities

(Figs. 4 and 5). The markedly lower $\Delta^{14}C$ values of both isoGDGTs and brGDGTs at depth would require that both groups of precursor organisms, i.e., archaea and bacteria, occupy specific niches using metabolic strategies that enable them to utilize stabilized, aged carbon. The precursor organisms of isoGDGTs in soils are known to be mainly comprised of Crenarchaeota, i.e., chemoautotrophic nitrifiers using soil CO_2 as substrate (Leininger et al., 2006; Urich et al., 2008; Weijers et al., 2010; Sinninghe Damsté et al., 2012) and acetotrophic methanogens (Weijers et al., 2010). Contributions from the latter organisms in the studied soils are likely minor as the soils are not strictly anaerobic Walthert, 2003). This is also supported by GDGT-0 / Crenarchaeol ratios that differ sharply from those in soils and sediments dominated by Thaumarchaeota (Blaga et al., 2009; Weijers et al., 2010; Naeher et al., 2014). Soil-respired CO_2 has relatively high $\Delta^{14}C$ values (Gaudinski et al., 2000; Liu et al., 2006), and thus it seems highly unlikely that ^{14}C-depleted signatures of isoGDGTs in the deeper soils results from metabolism of an old C substrate by active soil microbial communities. By analogy, the ^{14}C-depleted characteristics of brGDGTs is difficult to reconcile with heterotrophic consumption of preaged C. Overall, the contrasting metabolisms of the GDGT precursor organisms (primarily autotrophy for isoGDGTs and heterotrophy for brGDGTs), yet similar (and low) $\Delta^{14}C$ values for both compound classes, argue against an origin of the GDGT signals from microbial growth at depth. We therefore conclude that uptake of preaged carbon by active soil microbial communities is unlikely to be the cause for the ^{14}C-depleted GDGT signatures.

We next consider the long-term stabilization microbially derived carbon as the source of ^{14}C-depleted GDGT signatures. This implies that microbial residues persist in soils for millennia, lending support to emerging concepts that microbial necromass comprises an important component of older SOM (e.g., Lehmann and Kleber, 2015; Liang et al., 2017). Long-term persistence of GDGTs could arise from their stabilization by soil minerals at greater soil depths. The amphiphilic nature of lipids, such as GDGTs with both polar and hydrophobic components, promotes the association with mineral surfaces and therefore may afford physical protection from degradation (Jandl et al., 2004; Kleber et al., 2007; von Lützow et al., 2008; Van der Voort et al., 2017). By comparison, in surface soils with high organic matter contents and less availability of reactive mineral surfaces, GDGTs are continuously produced and degraded, which results in a younger mean radiocarbon age and evidence for turnover on decadal timescales (Weijers et al., 2010). This explanation agrees with conceptual models of soil organic matter dynamics, whereby older SOM in deeper soils primarily consists of microbial metabolites that are stabilized by their interaction with mineral surfaces (Schmidt et al., 2011; Lehmann and Kleber, 2015). Given the structural resemblance between brGDGTs and isoGDGTs, and hence similar propensity to associate with mineral surfaces, we consider this a more likely explanation for their similarly old ^{14}C ages than niche metabolisms of different precursor organisms. The older GDGT ^{14}C age in the lowest depth interval of the Cambisol at Lausanne compared to the sub-Alpine podzol at Beatenberg with a bleached eluvial horizon also supports this conclusion. The Lausanne soil has higher contents of clay and highly reactive amorphous Fe and Al oxides and hydroxides (Table 2), which are known to play a key role in the sorptive stabilization of SOM (Kaiser and Guggenberger, 2003; Kleber et al., 2007).

The ^{14}C signatures of GDGTs are similar in the top 20 cm at both locations (Fig. 4); however, in the Lausanne soil, the alkanes and fatty acids are less depleted in ^{14}C compared to Beatenberg, resulting in an offset between GDGTs and the plant-derived compounds. One explanation could be the different thicknesses of the organic layer at the two sites (Walthert, 2003). The 20 cm thick organic layer at Beatenberg retards the inputs of plant-derived C into the mineral soil and thus leads to longer turnover times of bulk OC in the topsoil compared to Lausanne, where the organic layer is only 2 to 3 cm thick. Contrary to the plant wax components, the turnover of isoGDGTs and brGDGTs does not seem to be affected by the thickness of the organic layer, resulting in the greater age offset observed in the Lausanne soil.

Overall, ^{14}C characteristics of iso- and brGDGTs and the inferred turnover times that are far longer than those of discrete POM (free light density fraction) and signature lipids of active microbial communities (short-chained fatty acids), but similar to those of plant-derived long-chain *n*-alkanes and fatty acids (Fig. 5), serve as strong evidence for the presence of mineral-stabilized microbial necromass in the studied forested mineral soils.

4.3 Implications for application of GDGTs as molecular proxies and soil tracer biomolecules

The relative abundance of different brGDGTs, as expressed in the MBT'_{5Me} and CBT' index values, correlates with MAT and soil pH (Weijers et al., 2007). The changing proportions of the individual brGDGTs reflected in both soils in the increasing CBT' index and, in the Beatenberg soil, decreasing MBT'_{5Me} index with depth correspond to a pH change from 4.6 to 5.7 in Lausanne and 4.8 to 5 in Beatenberg, while in the latter the reconstructed MAT decreases from 10.9 to 9.5 °C. In Beatenberg, these reconstructed values do not match the measured pH change from 3.7 to 4.4 with depth or reflect the MAT of 4.6 °C. Nevertheless, the direction of the changes, the increase in pH and the decrease in temperature with depth is echoed in the relative abundance of GDGTs. In Lausanne, however, the brGDGT-based increase in pH is not observed in the soil values, with measured pH remaining largely invariant (4.6 to 4.5) throughout the profile. Therefore, the significant increase in the CBT' index and hence the higher relative proportion of brGDGTs with cyclopentane moieties might reflect preferential association of these compounds to min-

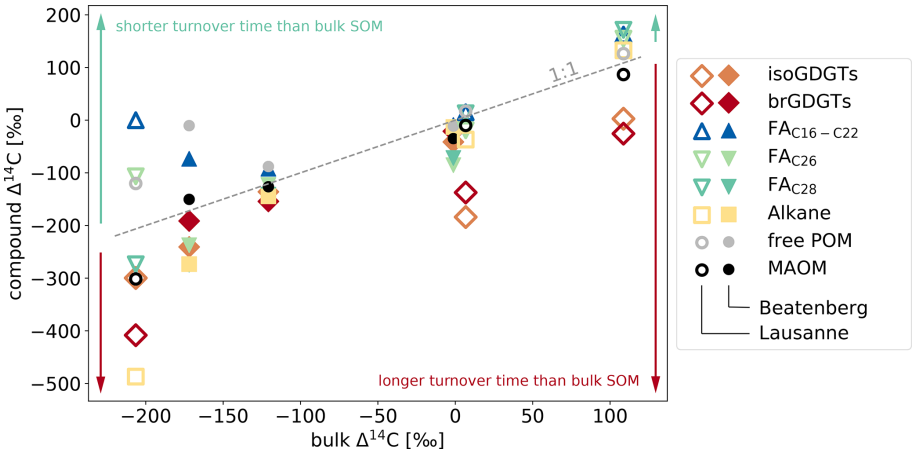

Figure 5. Relationship between $\Delta^{14}C$ values of specific components and bulk SOM in Beatenberg and Lausanne soil profiles. The different analyzed compounds and density fractions (Van der Voort et al., 2017) cover a greater range of $\Delta^{14}C$ values with soil depth, as reflected in the aging of the bulk OC in the respective soil. The dotted line represents equal compound and bulk $\Delta^{14}C$. Two groups are discernable, namely those with $\Delta^{14}C$ values higher than the bulk OC, and thus with a more rapid turnover (in most samples, this includes short-chain, i.e., C_{16}–C_{22}, FA and the low density fraction or free POM), and those with lower $\Delta^{14}C$ values, implying longer turnover times (including long-chain *n*-alkanes, i.e., in the Beatenberg soil C_{29}-alkane and in the Lausanne soil the C_{27}), and fatty acids, i.e., C_{26}, C_{28} FA, and the GDGTs.

Table 2. Soil properties related to the stability of soil organic matter. Effective cation exchange capacity (CEC), Fe_d (dithionite-extractable iron), Fe_o and Al_o (oxalate-extractable iron and aluminum), Fe_p and Al_p (pyrophosphate-extractable iron and aluminum) as well as sand, silt and clay content are provided by Zimmermann et al. (2006). Note: ppm – parts per million.

Loc	Depth	CEC (mmolC kg^{-1})	Fe_d (ppm)	Fe_o (ppm)	Fe_p (ppm)	Al_o (ppm)	Al_p (ppm)	Sand (%)	Silt (%)	Clay (%)
Bb	0–5 cm	50	1047	684	505	538	571	84	7	8
	10–20 cm	15	na	133	99	280	268	83	15	3
	20–40 cm	37	5770	2183	2062	880	1713	80	14	6
Ln	0–5 cm	77	6187	3356	2900	1861	1304	62	25	13
	10–20 cm	61	6493	3039	2310	2030	1430	51	31	18
	60–80 cm	59	5840	2095	732	1156	791	57	27	16

eral surfaces compared to those without cyclization. Further work is needed to ascertain whether some GDGT structures are more prone to protection by mineral association than others, as a change in relative abundance of brGDGTs with time due to different turnover of individual GDGTs would need to be considered when using brGDGTs to reconstruct environmental conditions.

In addition to the insights into soil carbon turnover, the observed ^{14}C signatures of GDGTs in the two soil profiles carry implications for their application as proxies of environmental conditions and as tracers of soil carbon input to aquatic environments. The putative application of brGDGTs as soil tracers has been undermined by the growing evidence pointing towards in situ production as a major source of brGDGTs in aquatic environments (e.g., De Jonge et al., 2014b; Sinninghe Damsté, 2016; Miller et al., 2018; Guo et al., 2020). Nevertheless, prior analyses of branched GDGTs in sedimentary archives have revealed older GDGT ages than depositional ages (Smittenberg et al., 2005; Birkholz et al., 2013), consistent with a contribution of aged brGDGTs that were subjected to protracted storage in and mobilization from deeper mineral soils.

5 Conclusions

We modified and validated a normal-phase HPLC method to isolate isoprenoid and branched GDGTs at the compound class level for radiocarbon analysis. Although further refinements in the method would be desirable, this new approach yields reliable GDGT ^{14}C measurements on sample sizes $> 20\,\mu g\,C$ that have enabled novel questions to be addressed concerning the provenance and turnover of this key suite of microbial lipids. In addition to its application to questions of soil C cycling, the streamlined method opens up new opportunities to further explore the biogeochemical and paleo-

climate significance of this intriguing yet enigmatic class of lipids.

Application of the method to depth profiles for two well-studied sub-Alpine soil profiles in Switzerland reveals a marked decrease in ^{14}C contents of both isoGDGTs and brGDGTs with depth, with resulting model estimates for GDGT turnover times of 2000 to 6000 years in deeper mineral soils. These old ages for archaeal and bacterial membrane lipids provide compelling evidence for stabilization of microbial necromass in soils that contributes to the long-term C storage. Through comparison with parallel ^{14}C data for soil density fractions and other hydrophobic lipid biomarkers, we attribute the stability of GDGTs to protection via association with reactive mineral surfaces, underlining the crucial role of microbial processes in soil C cycling and stabilization.

Our findings also provide motivation for further work to validate our interpretations and assess the broader significance of the current limited suite of observations. For example, comparison of the proportions and isotopic signatures of intact polar lipid GDGTs relative to the core lipids measured here could shed light on the significance active GDGT-producing communities residing at a specific soil depth versus remnants of past microbial activity (necromass). The potential sorptive stabilization of GDGTs could be verified by measuring GDGTs and their ^{14}C contents directly in mineral-protected OM (Mikutta et al., 2006); however, the low concentration of GDGTs could hamper this analysis. Furthermore, while concentrations of isoprenoid and branched GDGTs commonly decrease with increasing soil depth (Huguet et al., 2010; Yamamoto et al., 2016; Gocke et al., 2017), subsurface maxima in iso- and brGDGT concentrations have also been reported (Huguet et al., 2010; Yamamoto et al., 2016), potentially indicating depth-localized GDGT production. Future ^{14}C analysis of GDGTs in soil profiles that exhibit such subsurface concentration peaks would be informative and provide context for our observations in the two Swiss soil profiles. Further insights into the provenance and turnover of brGDGTs might be gained from an in-depth assessment of molecular distributions and associated proxy indices (De Jonge et al., 2014a), that may reflect changes in current or past microbial communities, or imply differences in susceptibility to degradation. Despite the presence of GDGTs as trace constituents of SOM, their unequivocal microbial origin, distinctive chemical structures and environmental properties that their distributions encode render them powerful tracer compounds and molecular proxies. Here we demonstrate that, when also constrained with natural abundance ^{14}C, these compounds provide a new window into the role of microorganisms in soil carbon cycling.

Appendix A

isoprenoid GDGTs

Name	m/z
Crenarchaeol	1292
Crenarchaeol'	1292'
GDGT - 0	1302
GDGT - 1	1300
GDGT - 2	1298
GDGT - 3	1296

branched GDGTs

Name	6-methyl isomer	m/z
Ia		1022
Ib		1020
Ic		1018
IIa / IIa'		1036
IIb / IIb'		1034
IIc / IIc'		1032
IIIa / IIIa'		1050
IIIb / IIIb'		1048
IIIc / IIIc		1046

$$MBT'_{5Me} = \frac{Ia + Ib + Ic}{Ia + Ib + Ic + IIa + IIb + IIc + IIIa}$$

$$CBT' = \log_{10}\left(\frac{Ic + IIa' + IIb' + IIc' + IIIa' + IIIb' + IIIc'}{Ia + IIa + IIIa}\right)$$

Figure A1. Molecular structures of GDGTs analyzed in this study. The equations to determine the MBT'_{5Me} and CBT' indices are taken from De Jonge et al. (2014a).

Code and data availability. The data set and script for the turnover model used in this study are available at https://doi.org/10.3929/ethz-b-000430425 (Gies et al., 2020).

Author contributions. HG, ML and TE conceptualized the study. HG and DM designed the method. HG isolated the compounds and wrote the turnover model. NH performed the radiocarbon measurements. TSvdV provided the data. HG, FH, ML and TE interpreted the data. HG prepared the paper with contributions from all coauthors.

Competing interests. The authors declare that they have no conflict of interest.

Acknowledgements. We thank Urs Overhoff and Markus Neuroth from RWE Power AG, for providing the lignite sample, and Marco Griepentrog and Cindy de Jonge, for the helpful discussions. We thank the Laboratory for Ion Beam Physics (ETH) for supporting us with the accelerator mass spectrometry measurements. Finally, this paper benefited from the thoughtful comments of two anonymous reviewers.

Financial support. This research has been supported by the Schweizerischer Nationalfonds zur Förderung der Wissenschaftlichen Forschung (grant no. 184865).

Review statement. This paper was edited by Yakov Kuzyakov and reviewed by two anonymous referees.

References

Ahrens, B., Braakhekke, M. C., Guggenberger, G., Schrumpf, M., and Reichstein, M.: Contribution of sorption, DOC transport and microbial interactions to the 14C age of a soil organic carbon profile: Insights from a calibrated process model, Soil Biol. Biochem., 88, 390–402, 2015.

Amelung, W., Brodowski, S., Sandhage-Hofmann, A., and Bol, R.: Combining biomarker with stable isotope analyses for assessing the transformation and turnover of soil organic matter, Adv. Agron., 100, 155–250, 2008.

Battin, T. J., Luyssaert, S., Kaplan, L. A., Aufdenkampe, A. K., Richter, A., and Tranvik, L. J.: The boundless carbon cycle, Nat. Geosci., 2, 598–600, 2009.

Birkholz, A., Smittenberg, R. H., Hajdas, I., Wacker, L., and Bernasconi, S. M.: Isolation and compound specific radiocarbon dating of terrigenous branched glycerol dialkyl glycerol tetraethers (brGDGTs), Organic geochemistry, 60, 9–19, 2013.

Blaga, C. I., Reichart, G.-J., Heiri, O., and Damsté, J. S. S.: Tetraether membrane lipid distributions in water-column particulate matter and sediments: a study of 47 European lakes along a north-south transect, J. Paleolimnol., 41, 523–540, 2009.

Bradford, M. A., Wieder, W. R., Bonan, G. B., Fierer, N., Raymond, P. A., and Crowther, T. W.: Managing uncertainty in soil carbon feedbacks to climate change, Nat. Clim. Change, 6, 751–758, 2016.

Carvalhais, N., Forkel, M., Khomik, M., Bellarby, J., Jung, M., Migliavacca, M., Saatchi, S., Santoro, M., Thurner, M., Weber, U., Ahrens, B., Beer, C., Cescatti, A., Randerson, J. T., and Reichstein, M.: Global covariation of carbon turnover times with climate in terrestrial ecosystems, Nature, 514, 213–217, 2014.

Coffinet, S., Huguet, A., Williamson, D., Fosse, C., and Derenne, S.: Potential of GDGTs as a temperature proxy along an altitudinal transect at Mount Rungwe (Tanzania), Org. Geochem., 68, 82–89, 2014.

Colcord, D. E., Pearson, A., and Brassell, S. C.: Carbon isotopic composition of intact branched GDGT core lipids in Greenland lake sediments and soils, Org. Geochem., 110, 25–32, 2017.

Cotrufo, M. F., Soong, J. L., Horton, A. J., Campbell, E. E., Haddix, M. L., Wall, D. H., and Parton, W. J.: Formation of soil organic matter via biochemical and physical pathways of litter mass loss, Nat. Geos., 8, 776–779, 2015.

Courel, B., Schaeffer, P., Adam, P., Ertlen, D., Schwartz, D., Bernasconi, S., and Hajdas, I.: Analyse, isolement et datation au 14C de lipides dans les sols: l'exemple des tétraéthers de diglycérol, Collection EDYTEM, Cahiers de géographie, 18, 57–68, 2015.

De Jonge, C., Hopmans, E. C., Zell, C. I., Kim, J.-H., Schouten, S., and Damsté, J. S. S.: Occurrence and abundance of 6-methyl branched glycerol dialkyl glycerol tetraethers in soils: Implications for palaeoclimate reconstruction, Geochim. Cosmochim. Ac., 141, 97–112, 2014a.

De Jonge, C., Stadnitskaia, A., Hopmans, E. C., Cherkashov, G., Fedotov, A., and Damsté, J. S. S.: In situ produced branched glycerol dialkyl glycerol tetraethers in suspended particulate matter from the Yenisei River, Eastern Siberia, Geochim. Cosmochim. Ac., 125, 476–491, 2014b.

De Rosa, M. and Gambacorta, A.: The lipids of archaebacteria, Prog. Lipid Res., 27, 153–175, 1988.

Feng, X. and Simpson, M. J.: Temperature responses of individual soil organic matter components, J. Geophys. Res.-Biogeo., 113, https://doi.org/10.1029/2008JG000743, 2008.

Freymond, C. V., Peterse, F., Fischer, L. V., Filip, F., Giosan, L., and Eglinton, T. I.: Branched GDGT signals in fluvial sediments of the Danube River basin: Method comparison and longitudinal evolution, Org. Geochem., 103, 88–96, 2017.

Gaudinski, J., Trumbore, S., Davidson, E., Cook, A., Markewitz, D., and Richter, D.: The age of fine-root carbon in three forests of the eastern United States measured by radiocarbon, Oecologia, 129, 420–429, 2001.

Gaudinski, J. B., Trumbore, S. E., Davidson, E. A., and Zheng, S.: Soil carbon cycling in a temperate forest: radiocarbon-based estimates of residence times, sequestration rates and partitioning of fluxes, Biogeochemistry, 51, 33–69, 2000.

Gies, H., Hagedorn, F., Lupker, M., Montlucon, D., Haghipour, N., van der Voort, T., and Eglinton, T.: Data Set – Millennial-age GDGTs inforested mineral soils, https://doi.org/10.3929/ethz-b-000430425, 2020.

Gill, R. A. and Jackson, R. B.: Global patterns of root turnover for terrestrial ecosystems, New Phytol., 147, 13–31, 2000.

Gleixner, G.: Soil organic matter dynamics: a biological perspective derived from the use of compound-specific isotopes studies, Ecol. Res., 28, 683–695, 2013.

Gocke, M. I., Huguet, A., Derenne, S., Kolb, S., Dippold, M. A., and Wiesenberg, G. L.: Disentangling interactions between microbial communities and roots in deep subsoil, Sci. Total Environ., 575, 135–145, 2017.

Guo, J., Glendell, M., Meersmans, J., Kirkels, F., Middelburg, J. J., and Peterse, F.: Assessing branched tetraether lipids as tracers of soil organic carbon transport through the Carminowe Creek catchment (southwest England), Biogeosciences, 17, 3183–3201, https://doi.org/10.5194/bg-17-3183-2020, 2020.

Haghipour, N., Ausín, B., Usman, M. O., Ishikawa, N., Wacker, L., Welte, C., Ueda, K., and Eglinton, T. I.: Compound-Specific Radiocarbon Analysis by Elemental Analyzer-Accelerator Mass Spectrometry: Precision and Limitations, Anal. Chem., 91, 2042–2049, 2018.

Hammer, S. and Levin, I.: Monthly mean atmospheric Δ 14 CO_2 at Jungfraujoch and Schauinsland from 1986 to 2016, heiDATA, https://doi.org/10.11588/data/10100, 2017.

He, N. and Yu, G.: Stoichiometrical regulation of soil organic matter decomposition and its temperature sensitivity, Ecol. Evol., 6, 620–627, 2016.

Heumann, G. and Litt, T.: Stratigraphy and paleoecology of the Late Pliocene and Early Pleistocene in the open-cast mine Hambach (Lower Rhine Basin), Neth. J. Geosci., 81, 193–199, 2002.

Hopmans, E. C., Weijers, J. W., Schefuß, E., Herfort, L., Damsté, J. S. S., and Schouten, S.: A novel proxy for terrestrial organic matter in sediments based on branched and isoprenoid tetraether lipids, Earth Planet. Sci. Lett., 224, 107–116, 2004.

Hopmans, E. C., Schouten, S., and Damsté, J. S. S.: The effect of improved chromatography on GDGT-based palaeoproxies, Org. Geochem., 93, 1–6, 2016.

Hua, Q., Barbetti, M., and Rakowski, A. Z.: Atmospheric radiocarbon for the period 1950–2010, Radiocarbon, 55, 2059–2072, 2013.

Huang, Y., Li, B., Bryant, C., Bol, R., and Eglinton, G.: Radiocarbon dating of aliphatic hydrocarbons a new approach for dating passive-fraction carbon in soil horizons, Soil Sci. Soc. Am. J., 63, 1181–1187, 1999.

Huguet, A., Fosse, C., Metzger, P., Fritsch, E., and Derenne, S.: Occurrence and distribution of non-extractable glycerol dialkyl glycerol tetraethers in temperate and tropical podzol profiles, Org. Geochem., 41, 833–844, 2010.

Huguet, A., Gocke, M., Derenne, S., Fosse, C., and Wiesenberg, G. L.: Root-associated branched tetraether source microorganisms may reduce estimated paleotemperatures in subsoil, Chem. Geol., 356, 1–10, 2013.

Huguet, A., Meador, T. B., Laggoun-Défarge, F., Könneke, M., Wu, W., Derenne, S., and Hinrichs, K.-U.: Production rates of bacterial tetraether lipids and fatty acids in peatland under varying oxygen concentrations, Geochim. Cosmochim. Ac., 203, 103–116, 2017.

Huguet, C., Hopmans, E. C., Febo-Ayala, W., Thompson, D. H., Damsté, J. S. S., and Schouten, S.: An improved method to determine the absolute abundance of glycerol dibiphytanyl glycerol tetraether lipids, Org. Geochem., 37, 1036–1041, 2006.

Ingalls, A. E. and Pearson, A.: Compound-Specific Radiocarbon Analysis, Oceanography, 18, 18–31, 2005.

Ingalls, A. E., Shah, S. R., Hansman, R. L., Aluwihare, L. I., Santos, G. M., Druffel, E. R., and Pearson, A.: Quantifying archaeal community autotrophy in the mesopelagic ocean using natural radiocarbon, P. Natl. Acad. Sci., 103, 6442–6447, 2006.

Innes, J. L.: Theoretical and practical criteria for the selection of ecosystem monitoring plots in Swiss forests, Environ. Monit. Assess., 36, 271–294, 1995.

Jandl, G., Leinweber, P., Schulten, H.-R., and Eusterhues, K.: The concentrations of fatty acids in organo-mineral particle-size fractions of a Chernozem, Eur. J. Soil Sci., 55, 459–470, 2004.

Kaiser, K. and Guggenberger, G.: Mineral surfaces and soil organic matter, Eur. J. Soil Sci., 54, 219–236, 2003.

Kallenbach, C. M., Frey, S. D., and Grandy, A. S.: Direct evidence for microbial-derived soil organic matter formation and its ecophysiological controls, Nat. Commun., 7, 13630, https://doi.org/10.1038/nature13731, 2016.

Kästner, M. and Miltner, A.: SOM and microbes – What is left from microbial life, in: The future of soil carbon, edited by: Garcia, C., Nannipieri, P., and Hernandez, T., Academic Press, Cambridge, Massachusetts, USA, 125–163, https://doi.org/10.1016/B978-0-12-811687-6.00005-5, 2018.

Kleber, M., Sollins, P., and Sutton, R.: A conceptual model of organo-mineral interactions in soils: self-assembly of organic molecular fragments into zonal structures on mineral surfaces, Biogeochemistry, 85, 9–24, 2007.

Kramer, C. and Gleixner, G.: Variable use of plant-and soil-derived carbon by microorganisms in agricultural soils, Soil Biol. Biochem., 38, 3267–3278, 2006.

Kramer, C. and Gleixner, G.: Soil organic matter in soil depth profiles: distinct carbon preferences of microbial groups during carbon transformation, Soil Biol. Biochem., 40, 425–433, 2008.

Kramer, C., Trumbore, S., Fröberg, M., Dozal, L. M. C., Zhang, D., Xu, X., Santos, G. M., and Hanson, P. J.: Recent (< 4 year old) leaf litter is not a major source of microbial carbon in a temperate forest mineral soil, Soil Biol. Biochem., 42, 1028–1037, 2010.

Lehmann, J. and Kleber, M.: The contentious nature of soil organic matter, Nature, 528, 60–68, 2015.

Leininger, S., Urich, T., Schloter, M., Schwark, L., Qi, J., Nicol, G. W., Prosser, J. I., Schuster, S., and Schleper, C.: Archaea predominate among ammonia-oxidizing prokaryotes in soils, Nature, 442, 806–809, 2006.

Liang, C., Schimel, J. P., and Jastrow, J. D.: The importance of anabolism in microbial control over soil carbon storage, Nat. Microbiol., 2, 1–6, 2017.

Liang, C., Amelung, W., Lehmann, J., and Kästner, M.: Quantitative assessment of microbial necromass contribution to soil organic matter, Glob. Change Biol., 25, 3578–3590, 2019.

Liu, W., Moriizumi, J., Yamazawa, H., and Iida, T.: Depth profiles of radiocarbon and carbon isotopic compositions of organic matter and CO_2 in a forest soil, J. Environ. Radioactiv., 90, 210–223, 2006.

Liu, W., Wang, H., Zhang, C. L., Liu, Z., and He, Y.: Distribution of glycerol dialkyl glycerol tetraether lipids along an altitudinal transect on Mt. Xiangpi, NE Qinghai-Tibetan Plateau, China, Org. Geochem., 57, 76–83, 2013.

Ma, T., Zhu, S., Wang, Z., Chen, D., Dai, G., Feng, B., Su, X., Hu, H., Li, K., Han, W., Liang, C., Bai, Y., and Feng, X.: Divergent accumulation of microbial necromass and plant lignin components in grassland soils, Nature Commun., 9, 1–9, 2018.

Matsumoto, K., Kawamura, K., Uchida, M., and Shibata, Y.: Radiocarbon content and stable carbon isotopic ratios of individual fatty acids in subsurface soil: Implication for selective microbial degradation and modification of soil organic matter, Geochem. J., 41, 483–492, 2007.

Mendez-Millan, M., Tu, T. N., Balesdent, J., Derenne, S., Derrien, D., Egasse, C., M'Bou, A. T., Zeller, B., and Hatté, C.: Compound-specific 13 C and 14 C measurements improve the understanding of soil organic matter dynamics, Biogeochemistry, 118, 205–223, 2014.

Mikutta, R., Kleber, M., Torn, M. S., and Jahn, R.: Stabilization of soil organic matter: association with minerals or chemical recalcitrance?, Biogeochemistry, 77, 25–56, 2006.

Miller, D. R., Habicht, M. H., Keisling, B. A., Castañeda, I. S., and Bradley, R. S.: A 900-year New England temperature reconstruction from in situ seasonally produced branched glycerol dialkyl glycerol tetraethers (brGDGTs), Clim. Past, 14, 1653–1667, https://doi.org/10.5194/cp-14-1653-2018, 2018.

Miltner, A., Bombach, P., Schmidt-Brücken, B., and Kästner, M.: SOM genesis: microbial biomass as a significant source, Biogeochemistry, 111, 41–55, 2012.

Mollenhauer, G., Inthorn, M., Vogt, T., Zabel, M., Sinninghe Damsté, J. S., and Eglinton, T. I.: Aging of marine organic matter during cross-shelf lateral transport in the Benguela upwelling system revealed by compound-specific radiocarbon dating, Geochem. Geophy. Geosy., 8, 1–9, https://doi.org/10.1038/s41467-018-05891-1, 2007.

Mollenhauer, G., Eglinton, T. I., Hopmans, E. C., and Damsté, J. S. S.: A radiocarbon-based assessment of the preservation characteristics of crenarchaeol and alkenones from continental margin sediments, Org. Geochem., 39, 1039–1045, 2008.

Naafs, B., Gallego-Sala, A., Inglis, G., and Pancost, R.: Refining the global branched glycerol dialkyl glycerol tetraether (brGDGT) soil temperature calibration, Org. Geochem., 106, 48–56, 2017.

Naeher, S., Peterse, F., Smittenberg, R. H., Niemann, H., Zigah, P. K., and Schubert, C. J.: Sources of glycerol dialkyl glycerol tetraethers (GDGTs) in catchment soils, water column and sediments of Lake Rotsee (Switzerland) – Implications for the application of GDGT-based proxies for lakes, Org. Geochem., 66, 164–173, 2014.

Oppermann, B., Michaelis, W., Blumenberg, M., Frerichs, J., Schulz, H.-M., Schippers, A., Beaubien, S., and Krüger, M.: Soil microbial community changes as a result of long-term exposure to a natural CO_2 vent, Geochim. Cosmochim. Ac., 74, 2697–2716, 2010.

Pancost, R. D. and Damsté, J. S. S.: Carbon isotopic compositions of prokaryotic lipids as tracers of carbon cycling in diverse settings, Chem. Geol., 195, 29–58, 2003.

Parry, M., Parry, M. L., Canziani, O., Palutikof, J., Van der Linden, P., and Hanson, C.: Climate change 2007 – impacts, adaptation and vulnerability: Working group II contribution to the fourth assessment report of the IPCC, vol. 4, Cambridge University Press, Cambridge, UK, 2007.

Pearson, A., McNichol, A. P., Benitez-Nelson, B. C., Hayes, J. M., and Eglinton, T. I.: Origins of lipid biomarkers in Santa Monica Basin surface sediment: a case study using compound-specific Δ 14 C analysis, Geochim. Cosmochim. Ac., 65, 3123–3137, 2001.

Peterse, F., van der Meer, J., Schouten, S., Weijers, J. W., Fierer, N., Jackson, R. B., Kim, J.-H., and Damsté, J. S. S.: Revised calibration of the MBT-CBT paleotemperature proxy based on branched tetraether membrane lipids in surface soils, Geochim. Cosmochim. Ac., 96, 215–229, 2012.

Powers, L., Werne, J. P., Vanderwoude, A. J., Damsté, J. S. S., Hopmans, E. C., and Schouten, S.: Applicability and calibration of the TEX86 paleothermometer in lakes, Org. Geochem., 41, 404–413, 2010.

Powers, L. A., Werne, J. P., Johnson, T. C., Hopmans, E. C., Damsté, J. S. S., and Schouten, S.: Crenarchaeotal membrane lipids in lake sediments: a new paleotemperature proxy for continental paleoclimate reconstruction?, Geology, 32, 613–616, 2004.

Riley, W. J., Maggi, F., Kleber, M., Torn, M. S., Tang, J. Y., Dwivedi, D., and Guerry, N.: Long residence times of rapidly decomposable soil organic matter: application of a multi-phase, multi-component, and vertically resolved model (BAMS1) to soil carbon dynamics, Geosci. Model Dev., 7, 1335–1355, https://doi.org/10.5194/gmd-7-1335-2014, 2014.

Ruff, M., Wacker, L., Gäggeler, H., Suter, M., Synal, H.-A., and Szidat, S.: A gas ion source for radiocarbon measurements at 200 kV, Radiocarbon, 49, 307–314, 2007.

Rumpel, C. and Kögel-Knabner, I.: Deep soil organic matter – a key but poorly understood component of terrestrial C cycle, Plant soil, 338, 143–158, 2011.

Schmidt, M. W., Torn, M. S., Abiven, S., Dittmar, T., Guggenberger, G., Janssens, I. A., Kleber, M., Kögel-Knabner, I., Lehmann, J., Manning, D. A., Nannipieri, P., Rasse, D. P., Weiner, S., and Trumbore, S. E.: Persistence of soil organic matter as an ecosystem property, Nature, 478, 49–56, 2011.

Schouten, S., Hopmans, E. C., Schefuß, E., and Sinninghe Damste, J. S.: Distributional variations in marine crenarchaeotal membrane lipids: a new tool for reconstructing ancient sea water temperatures?, Earth Planet. Sci. Lett., 204, 265–274, 2002.

Schouten, S., Hopmans, E. C., and Sinninghe Damste, J. S.: The organic geochemistry of glycerol dialkyl glycerol tetraether lipids: a review, Org. Geochem., 54, 19–61, 2013.

Schrumpf, M. and Kaiser, K.: Large differences in estimates of soil organic carbon turnover in density fractions by using single and repeated radiocarbon inventories, Geoderma, 239, 168–178, 2015.

Shah, S. R. and Pearson, A.: Ultra-microscale (5–25 µg C) analysis of individual lipids by 14 C AMS: Assessment and correction for sample processing blanks, Radiocarbon, 49, 69–82, 2007.

Shah, S. R., Mollenhauer, G., Ohkouchi, N., Eglinton, T. I., and Pearson, A.: Origins of archaeal tetraether lipids in sediments: Insights from radiocarbon analysis, Geochim. Cosmochim. Ac., 72, 4577–4594, 2008.

Sinninghe Damsté, J. S.: Spatial heterogeneity of sources of branched tetraethers in shelf systems: The geochemistry of tetraethers in the Berau River delta (Kalimantan, Indonesia), Geochim. Cosmochim. Ac., 186, 13–31, 2016.

Sinninghe Damsté, J. S., Rijpstra, W. I. C., Hopmans, E. C., Weijers, J. W., Foesel, B. U., Overmann, J., and Dedysh, S. N.: 13, 16-Dimethyl octacosanedioic acid (iso-diabolic acid), a common membrane-spanning lipid of Acidobacteria subdivisions 1 and 3, Appl. Environ. Microb., 77, 4147–4154, 2011.

Sinninghe Damsté, J. S., Rijpstra, W. I. C., Hopmans, E. C., Jung, M.-Y., Kim, J.-G., Rhee, S.-K., Stieglmeier, M., and Schleper, C.: Intact polar and core glycerol dibiphytanyl glycerol tetraether

lipids of group I. 1a and I. 1b Thaumarchaeota in soil, Appl. Environ. Microb., 78, 6866–6874, 2012.

Sinninghe Damsté, J. S., Rijpstra, W. I. C., Foesel, B. U., Huber, K. J., Overmann, J., Nakagawa, S., Kim, J. J., Dunfield, P. F., Dedysh, S. N., and Villanueva, L.: An overview of the occurrence of ether-and ester-linked iso-diabolic acid membrane lipids in microbial cultures of the Acidobacteria: Implications for brGDGT paleoproxies for temperature and pH, Org. Geochem., 124, 63–76, 2018.

Smittenberg, R. H., Hopmans, E. C., Schouten, S., and Damsté, J. S. S.: Rapid isolation of biomarkers for compound specific radiocarbon dating using high-performance liquid chromatography and flow injection analysis – atmospheric pressure chemical ionisation mass spectrometry, J. Chromatogr. A, 978, 129–140, 2002.

Smittenberg, R. H., Hopmans, E. C., Schouten, S., Hayes, J. M., Eglinton, T. I., and Sinninghe Damste, J. S.: Compound-specific radiocarbon dating of the varved Holocene sedimentary record of Saanich Inlet, Canada, Paleoceanography, 19, https://doi.org/10.1029/2003PA000927, 2004.

Smittenberg, R. H., Baas, M., Green, M. J., Hopmans, E. C., Schouten, S., and Damsté, J. S.: Pre-and post-industrial environmental changes as revealed by the biogeochemical sedimentary record of Drammensfjord, Norway, Mar. Geol., 214, 177–200, 2005.

Sollins, P., Homann, P., and Caldwell, B. A.: Stabilization and destabilization of soil organic matter: mechanisms and controls, Geoderma, 74, 65–105, 1996.

Solly, E. F., Brunner, I., Helmisaari, H.-S., Herzog, C., Leppälammi-Kujansuu, J., Schöning, I., Schrumpf, M., Schweingruber, F. H., Trumbore, S. E., and Hagedorn, F.: Unravelling the age of fine roots of temperate and boreal forests, Nat. Commun., 9, 1–8, 2018.

Synal, H., Stocker, M., and Suter, M.: Nuclear Instruments and Methods in Physics Research Section B-Beam 389, Interactions with Materials and Atoms, 259, 7–13, 2007.

Torn, M., Swanston, C., Castanha, C., and Trumbore, S.: Storage and turnover of organic matter in soil, in: Biophysico-chemical processes involving natural nonliving organic matter in environmental systems, edited by: Senesi, N., Xing, B., and Huang, P. M., chap. 6, 219–272, Wiley, Hoboken, NJ, USA, https://doi.org/10.1002/9780470494950.ch6, 2009.

Trumbore, S.: Age of soil organic matter and soil respiration: radiocarbon constraints on belowground C dynamics, Ecol. Appl., 10, 399–411, 2000.

Trumbore, S. E., Chadwick, O. A., and Amundson, R.: Rapid exchange between soil carbon and atmospheric carbon dioxide driven by temperature change, Science, 272, 393–396, 1996.

Tunlid, A. and White, D. C.: Biochemical Analysis Of Biomass, Community Structure, Nutritional Status, and Metabolic Activity, in: SoilBiochemistry, edited by: Stotzky, G. and Bollag, J. M., vol. 7, 229–262, Marcel Dekker, New York, NY, USA, 1991.

Urich, T., Lanzén, A., Qi, J., Huson, D. H., Schleper, C., and Schuster, S. C.: Simultaneous assessment of soil microbial community structure and function through analysis of the meta-transcriptome, PloS one, 3, https://doi.org/10.1371/journal.pone.0002527, 2008.

van der Voort, T. S., Hagedorn, F., McIntyre, C., Zell, C., Walthert, L., Schleppi, P., Feng, X., and Eglinton, T. I.: Variability in ^{14}C contents of soil organic matter at the plot and regional scale across climatic and geologic gradients, Biogeosciences, 13, 3427–3439, https://doi.org/10.5194/bg-13-3427-2016, 2016.

Van der Voort, T. S., Zell, C., Hagedorn, F., Feng, X., McIntyre, C. P., Haghipour, N., Graf Pannatier, E., and Eglinton, T. I.: Diverse soil carbon dynamics expressed at the molecular level, Geophys. Res. Lett., 44, 11840–11850, 2017.

van der Voort, T. S., Mannu, U., Hagedorn, F., McIntyre, C., Walthert, L., Schleppi, P., Haghipour, N., and Eglinton, T. I.: Dynamics of deep soil carbon – insights from ^{14}C time series across a climatic gradient, Biogeosciences, 16, 3233–3246, https://doi.org/10.5194/bg-16-3233-2019, 2019.

von Lützow, M., Kögel-Knabner, I., Ludwig, B., Matzner, E., Flessa, H., Ekschmitt, K., Guggenberger, G., Marschner, B., and Kalbitz, K.: Stabilization mechanisms of organic matter in four temperate soils: Development and application of a conceptual model, J. Plant Nutr. Soil Sc., 171, 111–124, 2008.

Walthert, L.: Langfristige Waldökosystem-Forschung LWF in der Schweiz, Kernprojekt Bodenmatrix: Ergebnisse der ersten Erhebung 1994–1999, Tech. rep., ETH Zurich, Zurich, Switzerland, 154 pp., 2003.

Weber, Y., De Jonge, C., Rijpstra, W. I. C., Hopmans, E. C., Stadnitskaia, A., Schubert, C. J., Lehmann, M. F., Sinninghe Damste, J. S., and Niemann, H.: Identification and carbon isotope composition of a novel branched GDGT isomer in lake sediments: Evidence for lacustrine branched GDGT production, Geochim. Cosmochim. Ac., 154, 118–129, 2015.

Weijers, J. W., Schouten, S., Hopmans, E. C., Geenevasen, J. A., David, O. R., Coleman, J. M., Pancost, R. D., and Sinninghe Damsté, J. S.: Membrane lipids of mesophilic anaerobic bacteria thriving in peats have typical archaeal traits, Environ. Microbiol., 8, 648–657, 2006a.

Weijers, J. W., Schouten, S., Spaargaren, O. C., and Damsté, J. S. S.: Occurrence and distribution of tetraether membrane lipids in soils: Implications for the use of the TEX86 proxy and the BIT index, Org. Geochem., 37, 1680–1693, 2006b.

Weijers, J. W., Schouten, S., van den Donker, J. C., Hopmans, E. C., and Damsté, J. S. S.: Environmental controls on bacterial tetraether membrane lipid distribution in soils, Geochim. Cosmochim. Ac., 71, 703–713, 2007.

Weijers, J. W., Panoto, E., van Bleijswijk, J., Schouten, S., Rijpstra, W. I. C., Balk, M., Stams, A. J., and Sinninghe Damste, J. S.: Constraints on the biological source (s) of the orphan branched tetraether membrane lipids, Geomicrobiol. J., 26, 402–414, 2009.

Weijers, J. W. H., Wiesenberg, G. L. B., Bol, R., Hopmans, E. C., and Pancost, R. D.: Carbon isotopic composition of branched tetraether membrane lipids in soils suggest a rapid turnover and a heterotrophic life style of their source organism(s), Biogeosciences, 7, 2959–2973, https://doi.org/10.5194/bg-7-2959-2010, 2010.

Yamamoto, Y., Ajioka, T., and Yamamoto, M.: Climate reconstruction based on GDGT-based proxies in a paleosol sequence in Japan: Postdepositional effect on the estimation of air temperature, Quatern. Int., 397, 380–391, 2016.

Yang, H., Pancost, R. D., Jia, C., and Xie, S.: The response of archaeal tetraether membrane lipids in surface soils to temperature: a potential paleothermometer in paleosols, Geomicrobiol. J., 33, 98–109, 2016.

Zimmermann, S., Luster, J., Blaser, P., Walthert, L., and Lüscher, P.: Waldböden der Schweiz, Band 3, Regionen Mittelland und Vo-

ralpen, Swiss Federal Research Institute WSL, Hep Verlag Bern, Switzerland, 2006.